JOURNAL OF MATERIALS SCIENCE 25 (1990) 4324–4330

Electronic paramagnetic resonance (EPR) study of the structure of ZnO varistors prepared by various chemical methods

M. V. VLASOVA, N. G. KAKAZEY
The Institute for Problems of Materials Science of the Ukrainian Academy of Sciences, Kiev, USSR

O. MILOSEVIĊ, D. P. USKOKOVIĊ
The Institute of Technical Sciences of the Serbian Academy of Sciences and Arts, Belgrade

D. POLETI, D. VASOVIĊ
The Faculty of Technology and Metallurgy, Belgrade University, Belgrade, Yugoslavia

The structure of ZnO varistors prepared by different chemical methods was studied by the electronic paramagnetic resonance (EPR) method. The presence of Mn^{2+} ions in both ZnO lattice and electroconductive phase was used as a sensitive "probe" for the analyses of structural changes which occur during sintering of ZnO varistors. Potential mechanisms which can contribute to the formation of resonant lines were considered. The concentration of paramagnetic centres was quantitatively analysed. The variation of EPR signals of Mn^{2+} ions in ZnO phase was registered as a function of the chemical methods used for the preparation of powders only when samples were sintered at lower temperatures and non-linear characteristics of varistor ceramics had not yet been reached. At higher sintering temperatures EPR signals of Mn^{2+} ions in electroconductive phase differed only in the case of powders obtained by NaOH coprecipitation.

1. Introduction

Modern science of fine particle systems is based on the study of properties of materials formed at the boundary between particles of the same or different chemical composition. The study is limited because of the lack of a unique method for precise process control. A great number of different physical methods are used to obtain information about the properties of dispersed systems. The obtained data are either integral, characterizing the properties of the whole sample, or differential, describing the properties of some centres, defects, etc. The resonance methods give great possibilities for the investigation of differential properties. One of the most significant is the "resonance probe method" [1–3]. The role of the probe is played by one of the components present in the mixture or by an additive specially introduced into the mixture and reflects the structural rearrangement which occurs during sintering. We have already shown [4] that a Mn^{2+} ion entering into the lattice of ZnO and Bi_2O_3 phase represents a very "sensitive probe" which enabled us to follow the structural changes which occur during sintering of ZnO varistors.

Preparation of fine reactive powders of high purity and controlled composition and particle shape becomes the most important part of the production of varistors with very reliable ceramic and electric properties. The following chemical procedures used in the preparation of varistor ceramics have been described: the sol–gel [5], the evaporation of solutions and suspensions [6, 7], the coprecipitation [7, 8], and the evaporative decomposition of solution (EDS) [9, 10].

In this work electronic paramagnetic resonance (EPR) was used for the study of ZnO multicomponent varistors ceramics prepared by different chemical methods. The EPR technique can be applied in this case due to the presence of transition metal oxides (MnO_2, Cr_2O_3, NiO etc.) which act as the resonance probe.

2. Experiments

The mixture used for the synthesis of varistors contained 92.7 mol % of ZnO and 7.3 mol % of additives from the following group of compounds: $Co(NO_3)_2 \cdot 6H_2O$, $Ni(NO_3)_2 \cdot 6H_2O$, $Cr(NO_3)_2 \cdot 9H_2O$, $Bi(NO_3)_3 \cdot 5H_2O$, $Mn(CH_3COO)_2 \cdot 4H_2O$ and $SbCl_3$. Five initial mixtures named a, b, c, d and e were prepared.

Mixture a was prepared by adding a defined quantity of ZnO powder to a solution of additives. The obtained suspension was evaporated and dried at 423 K. It was found that the dominant phase, $Zn(OH)_8(NO_3)_2 2H_2O$, decomposed and the powder amorphized during prolonged drying. It was shown by TGA that the obtained powder decomposed in the temperature range 323 to 1043 K with a maximum weight loss of 39%. After thermogravimetric analysis we found diffraction maxima of ZnO and spinel phase and a phase

0022–2461/90 $03.00 + .12

of $Bi_{12}MnO_{20}$ type. The following calcination at 973 K in few hours resulted in a ZnO phase and slightly crystallized spinel.

Mixtures b and c were prepared in the same manner as the mixture a, but the whole quantity of zinc component was added in the form of $Zn(NO_3)_2$ solution (mixture c) or 40% was added as $Zn(NO_3)_2$ solution and 60% as solid ZnO powder (mixture b). The decomposition of both mixtures was done in a sand bath and the calcination occurred at 1073 K resulting in a ZnO phase and slightly crystallized spinel.

Mixture d was prepared by quantitative coprecipitation of additives solution with NaOH at pH = 10.10. The zinc component in the form of ZnO powder was added to the prepared solution. The weight loss of this mixture during TGA was very small (5% up to 1273 K), but the temperature of the final decomposition was higher. The X-ray analysis confirmed the presence of ZnO and a small quantity of a less ordered phase. The sample heated at 1273 K had a X-ray spectrum typical of sintered varistors i.e. ZnO phase, the spinel and β-Bi_2O_3 were observed. The calcination was done at 973 K.

Mixture e was obtained from the melt of crystallohydrated salts of all components, which were thermally dehydrated and decomposed at temperatures not higher than 973 K. Crystallized ZnO and the spinel with lower degree of crystallinity compared to the previous mixtures were observed by the X-ray technique.

In all calcinated mixtures two non-identified intermedial phases were found in a small quantity as the results of incomplete decomposition of the intermedial compounds. These phases were not registered in sintered samples.

The mean particle size of calcinated powders was 2.69, 1.23, 1.16, 1.20 and 0.90 μm, respectively.

After the calcination the powder was uniaxially pressed as discs of 8 mm diameter and 1 to 5 mm height. The porosity of the green discs was $\simeq 60\%$ of the theoretical density. The samples were sintered in the temperature range 1073 to 1573 K for one hour.

EPR spectra were recorded by 3 cm EPR radiospectrometer RE 13-06 at room and liquid nitrogen temperature. For all measurements crushed samples were used because a relatively high electrical conductivity made EPR measurements on compact samples impossible.

3. Discussion

3.1. Theory of Mn^{2+} signals in ZnO

The already known EPR signal of Mn^{2+} in ZnO [4] was registered in all samples at room temperature (Fig. 1). It may be described by the spin Hamiltonian

$$\mathcal{H} = g\beta BS + D\,[S_z^2 - \tfrac{1}{2}S(S+1)] + ASI \tag{1}$$

where g is the factor of spectroscopic splitting, β the Bohr magneton, S the effective electron spin operator, A the constant of the isotropic hyperfine interaction, B the induction of outward magnetic field, D the axial distortion parameter and I the effective nuclear spin operator. The obtained spectrum was the following parameters: $g = 2.0010 \pm 0.0005$; $D = 25.0 \pm 0.2$ mT; $A = 7.92 \pm 0.04$ mT. During measurements at 77 K, besides this spectrum, an asymmetric signal with $g = 4.27$ was also registered. It can be attributed to ions in s state which are in a strong rhombohedral deformed crystal field [11]. The basic measured parameters were: the amplitude of separated spectrum lines (I) across the unit sample weight and their width (ΔB).

In general case the angular relationship of the position of all fine structure lines ($\Delta M = 1, \Delta m = 0$) in the magnetic field, taking into account corrections for higher orders in the perturbation theory [12], may be given as

$$\begin{aligned} B(M \leftrightarrow M-1, m, \theta) &= B_0 - D(M - \tfrac{1}{2}) \\ &\times (3\cos^2\theta - 1) - \frac{D^2}{2B_0}\cos^2\theta \sin^2\theta \\ &\times [4S(S+1) - 24M(M-1) - 9] - \frac{D^2 \sin^4\theta}{8B_0} \\ &\times [2S(S+1) - 6M(M-1) - 3] \\ &- Am - \frac{A^2}{2B_0}[I(I+1) - m^2 + (2m-1)m] \\ &- \frac{D^2 A}{2B_0^2}\sin^2\theta\cos^2\theta \\ &\times \left(\frac{[M^2 - S(S+1)]^2 - M^2}{M} \right. \\ &\left. - \frac{[(M-1)^2 - S(S+1)]^2 - (M-1)^2}{M-1} \right) m \\ &- \frac{D^2 A}{8B_0^2}\sin^4\theta \{M[2M + 1 - 2S(S+1)] \\ &- (M-1)[2(M-1)^2 + 1 - 2S(S+1)]\} m \end{aligned} \tag{2}$$

where B_0 is the resonant value of outward magnetic field induction, M and m are quantum numbers of the momentum projection of electron and nuclear spin, respectively, θ is the angle between Z-crystal axes and magnetic field B.

In the case of polycrystalline samples the angle relationship is averaged and the registered spectrum represents the set of relatively narrow asymmetric lines singularities [11] whose position in the magnetic field is determined generally by the condition $[\nabla_\theta B(M \leftrightarrow M-1, m\ \theta)] = 0$. Applied on the particular case, the position of the most intensive singularities is determined by the condition $\sin\theta / \mathrm{d}B(\theta)/\mathrm{d}\theta \to \infty$. The equation for the singularity position in the case of Mn^{2+} spectrum in ZnO has been already given [4], enabling the determination of constants of the spin Hamiltonian.

Using computer analyses of anisotropic EPR signals which also have anisotropic line widths, it was possible to obtain line widths of the crystal in the orientation of predicted singularity position [13].

The change of conditions of sample preparation often results in the change of mechanisms which participate in the formation of resonant signals. It is of

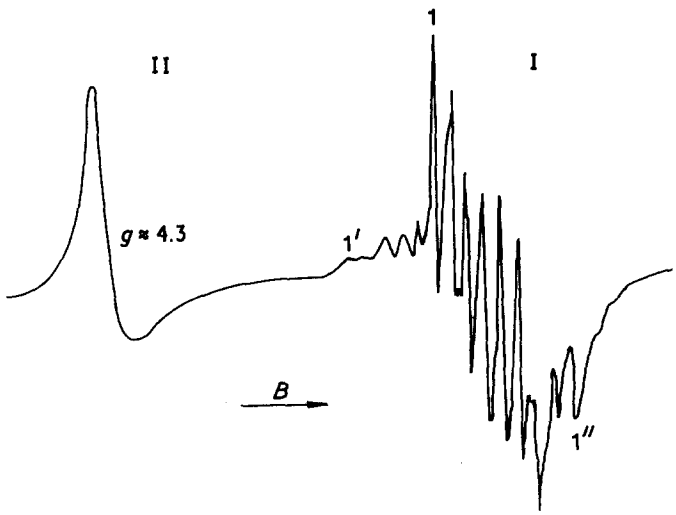

Figure 1 General shape of EPR spectrum of mixture c. Sintering temperature – 1373 K; EPR measurement temperature – 77 K. 1, 1' and 1''-transition singularities – 1/2, $-5/2 \leftrightarrow 1/2$, $-5/2$ ($\theta = 90°$); – 1/2, $-5/2 \leftrightarrow -3/2$, $-5/2$ ($\theta = 90°$); 1/2, $5/2 \leftrightarrow 3/2$, 5/2 ($\theta = 90°$) respectively; I Mn^{2+} in ZnO; II Mn^{2+} in electroconductive phase.

significant interest to explain the particular mechanisms of broadening. The basic mechansims that may be important in the analysed case are

(a) The deformation of the crystal field around paramagnetic centres on account of lattice defects.

(b) The dipole–dipole interaction between paramagnetic centres during the increase of their content in the sample.

(c) The conduction electrons and paramagnetic centres interaction.

3.1.1. Deformation of crystal fields around paramagnetic centres on account of lattice defects

The presence of lattice defects (isovalent impurities in closer surroundings are also included) brings to the appearance of a set of paramagnetic spin Hamiltonian [1] for each paramagnetic centre in the sample i.e. the resulting signal in this case represents the superposition of signals of unit centres partially shifted. Compared to the defectless sample, the signal of the defected sample will be broadened [14].

The basic parameter, sensitive to the presence of lattice defects is the fine structure parameter D. Assuming that defects are distributed in the bulk statistically unordered (chaotically), it is easy to show that deviation D from D_0 has Gaussian characteristics and it may be described by the value ΔD. The existence of this deviation brings to the appearance of inhomogeneous broadening of the resulting resonance signal. Its contribution is given by

$$\Delta B_g = \frac{\partial B(M, \theta)}{\partial D} \Delta D = K_\theta \cdot \Delta D$$

It is obvious that ΔB_g is a function of the angle relationship. If the shape of an individual line in the non-deformed crystal is Lorentzian with widths ΔB_0, the width of the resulting signal in the deformed sample will be given by the following relationship [15]

$$\Delta B = \frac{\Delta B_0}{2} + \frac{\Delta B_0}{4} + \Delta B_g^2 \qquad (3)$$

or for individual lines of Gaussian shape

$$\Delta B^2 = \Delta B_0^2 + \Delta B_g^2 \qquad (4)$$

If the resonance line in non-deformed sample is not a function of the angle of signal width, it will have in it deformed sample. The EPR spectrum in a defect polycrystal may be considered from the standpoint of the mean signal, which is a function of the angle of both the position of magnetic field and its width and shape.

The calculated values of K_θ for different transitions to positions that correspond to singularities (θ_1 and θ_2) in the polycrystal sample are given in Table I. It is obvious that variations of K_θ are significant. It is possible to estimate ΔB_g and ΔD from the analysis of ΔB for different transitions. We have to emphasize again that various mechanisms which cause spectrum broadening because of lattice defects bring about different broadening of singularity connected either with various transitions or with various characteristic points of polycrystals (θ_1 and θ_2).

To estimate qualitative differences in defect structure it is recommended that the ratio of singularity amplitudes used then have significantly different coefficients of deformation broadening, K_θ.

3.1.2. Dipole–dipole interaction

The energy of the dipole–dipole interaction between paramagnetic centres of the same type is given by the spin Hamiltonian [16]

$$\mathcal{H}_{dd} = S(S + 1) \frac{g^2 \beta^2}{r^3} (1 - 3 \cos^2 \theta)$$

where r is the mean distance between centres.

In the first approximation the contribution of dipole–dipole broadening in various transitions is equal, i.e. if the width of various transitions in non-

TABLE I Calculated values of deformation broadening K_θ for singularity of different transitions in the spectrum of Mn^{2+} in ZnO

Transition		K_{θ_1}, $\theta = 90°$	θ_2	K_{θ_2}
$\pm 5/2$, m $\leftrightarrow \pm 3/2$, m		$\simeq 2$		
$\pm 3/2$, m $\leftrightarrow \pm 1/2$, m		$\simeq 1$		
	m			
	$-5/2$	0.6	42° 45′	0.41
$-1/2 \leftrightarrow +1/2$				
	$-3/2$	0.6	42° 30′	0.70
	$-1/2$	0.6	42° 5′	0.96
	1/2	0.6	41° 30′	1.19
	3/2	0.6	40° 45′	1.40
	5/2	0.6	39° 25′	1.57

deformed sample is different (usually $B_{\pm 5/2 \leftrightarrow \pm 3/2} > \Delta B_{\pm 3/2 \leftrightarrow \pm 1/2} > \Delta B_{-1/2 \leftrightarrow 1/2}$), with an increase in impurity content it will tend to the value for all transitions influenced mainly by dipole–dipole broadening.

3.1.3. Conduction electrons and paramagnetic centres interaction

In electroconductive systems on interaction occurs between charge carriers and localized spin centres and then

$$\mathscr{H} = JS_{cc}S_{pc}$$

where J is the exchange integral, S_{cc} the spin of charge carriers and S_{pc} the spin of paramagnetic centres. According to Koringa's law [17], the rate of relaxation of localized spins is proportional to the concentration of charge carriers. The time of the spin–spin relaxation of paramagnetic centres (t_2') is

$$\frac{1}{t_2'} = \frac{1}{t_2} + \frac{\pi}{h}[J\rho(E_F)]^2 kT$$

where t_2 is the time of spin–spin relaxation in samples without charge carriers, $\rho(E_F)$ the density of charge carriers at the Fermi level, T the temperature and k the Boltzmann constant. At relatively small values of the splitting parameter in the crystal field (which is also the case of Mn^{2+} in ZnO) the diminution in time of the spin–spin relaxation will have the same influence on different transitions of fine structures as the dipole broadening. The existence of temperature dependence $1/t_2'$ (line width) may be taken as the basis for the separation of the broadening which is the result of dipole–dipole interaction and the exchange mechanism, particularly in the case of semiconductors.

3.1.4. Quantitative analysis of the concentration of paramagnetic centre based on EPR spectra in polycrystalline samples

Usually the concentration of paramagnetic centres is determined by double integration of the resulting spectrum (after the EPR spectra are registered in the shape of differential signals of absorption) and by the comparison with the reference signal. It is easily done in the case of spectra consisting of a single line. Complex spectra in polycrystals become a problem not only because of the determination of absolute concentration, but also because of the relative concentration. The relative change of centres concentration can be estimated by the measurement of amplitudes of corresponding EPR spectra at the unchanged shape of the whole spectrum.

The case is more complex if the width (and the shape) of the singularity is significantly changed. The analysis of model EPR spectra of Mn^{2+} in polycrystals shows for systems with a wide choice of parameters [18] that the approach of individual lines $I\Delta B^2 =$ const can be applied for transitions $-1/2, m \leftrightarrow +1/2, m$ if $B_{\theta_1} - B_{\theta_2} < \Delta B$. For $(B_{\theta_1} - B_{\theta_2}) \gg \Delta B$ the relationship $I\Delta B =$ const can be used for the singularity. The first approach may be also followed by the second one for non-central transition at $\theta = 90°$ with the increase of line width.

We must also take into account the fact that the increase of ΔB results in the superposition of neighbouring transitions which introduce the deformation in the determination of both singularity and its amplitude.

For the qualitative estimation of the relative integral intensity of signals we used both approaches.

3.2. Analysis of experimental results

3.2.1. EPR spectrum of Mn^{2+} in ZnO

The response signal amplitude (I), the line width (ΔB) and "the conditional integral intensity" (J_{int}) of ZnO samples as functions of the sintering temperature are shown in Figs 2 to 4. Generally, the relationships are rather similar and some differences between samples prepared by different chemical methods were registered only at lower sintering temperatures.

Measurements at 77 K did not show any significant changes of the width and shape of the separate singularities. This confirms the responsibility of deformation and concentration reconstructions for the registered changes.

The general shape of the temperature change of the amplitude, the width and the integral intensity of EPR signals is in good agreement with the successive increase of additive concentration c in the function of sintering temperature. According to Kittel and Abrahams [16], for an increase of c up to 10% the width of the dipole–dipole line is proportional to the concentration i.e. $\Delta B_{dip} \simeq Kc$, where K is a constant. The width of the resulting signal must include ΔB in the sample without dipole broadening. Then, [3, 4]

$$\Delta B^2 = \Delta B_0^2 + \Delta B_{dip}^2 = \Delta B_0^2 + (Kc)^2$$

Since the integral intensity of the signal $J \simeq I\Delta B^2$ is

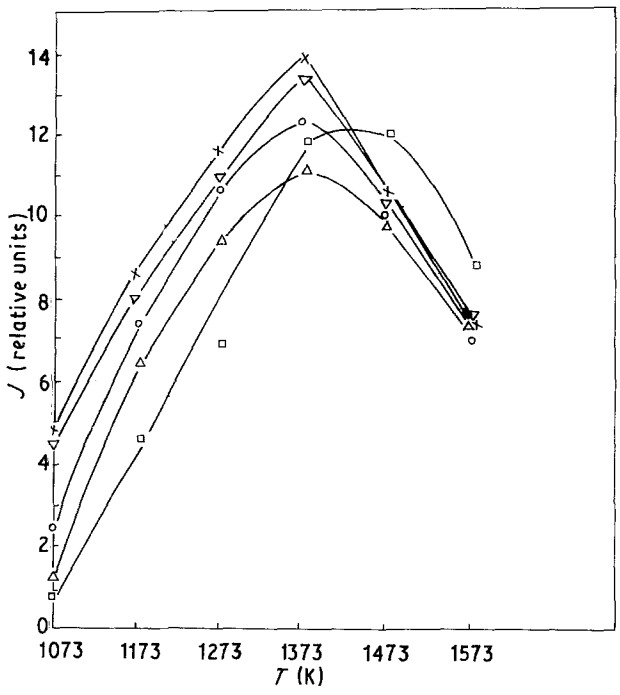

Figure 2 Singularity amplitude (I'') in EPR spectrum of Mn^{2+} in ZnO as the function of sintering temperatures for the investigated varistor systems. (○, a; ×, b; △, c; □, d; ▽, e)

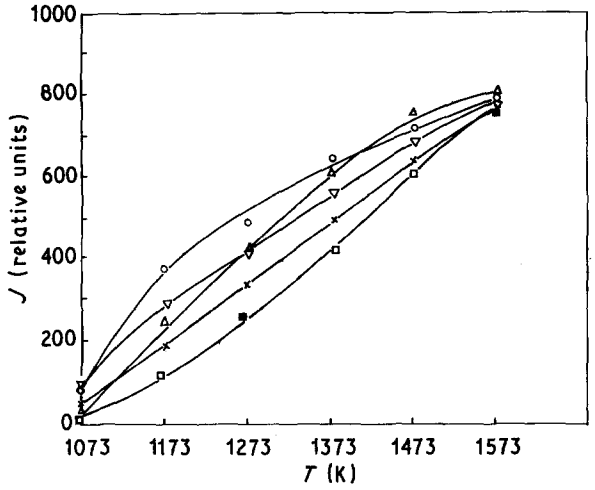

Figure 3 EPR singularity width (1″ and 1) in EPR spectrum of Mn^{2+} in ZnO as the function of sintering temperatures for the investigated varistor systems. Symbols as in Fig. 2.

proportional to the concentration c

$$I \sim \frac{c}{\Delta B_0^2 + (Kc)^2}$$

i.e. at low values of c the signal amplitude increases proportionally with the concentration ($I \sim c/\Delta B_0^2$) and at higher values ($Kc)^2 \gg B_0^2$) it decreases ($I \sim \frac{1}{2}$). The change of ΔB and J (Fig. 5) is in quite good agreement with this schedule.

For qualitative estimation of the defectness degree of the samples we can use the relationship between amplitudes of singularities I_1/I_2'' (Fig. 1) and sintering temperature (Fig. 6). According to the previous analysis a higher value of this ratio corresponds to a higher degree of sample defectness (if other conditions are the same). From this standpoint the most defective samples at 1073 K are system a ($\Delta D \simeq 2$ mT) and the most perfect are b and e. Over 1273 K a defect structure was not detected.

3.2.2. EPR signal with g = 4.27

The absence of other ions with basic s state indicates that Mn^{2+} ions are responsible for this signal. Generally it is possible to make conditions in the ZnO lattice for the stabilization of Mn^{2+} in the strong rhombic deformed field [11]. The existence of such

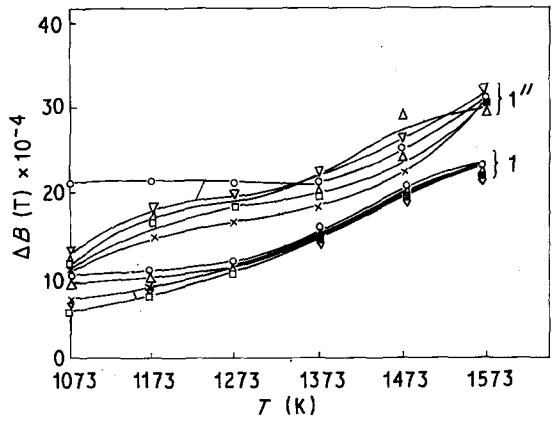

Figure 4 EPR spectrum (1″) intensity of Mn^{2+} in ZnO as the function of sintering temperatures for the investigated varistor systems. Symbols as in Fig. 2.

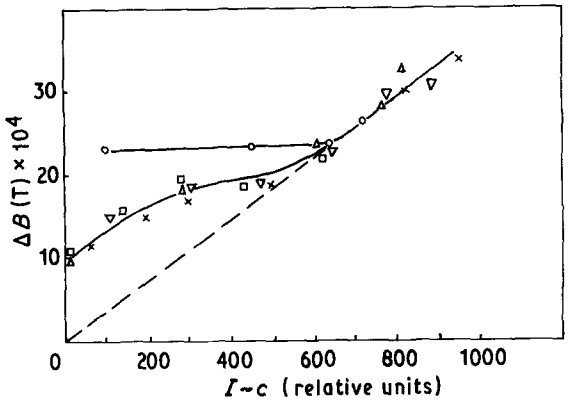

Figure 5 EPR singularity width (1″) in EPR spectrum of Mn^{2+} in ZnO as the function of concentration of Mn^{2+} ions. Symbols as in Fig. 2.

defects in ZnO would, however, be followed by their appearance in the basic spectrum of Mn^{2+} in ZnO as well. On the other hand impurities in the s state have long times of relaxation in most lattice types. The absence of such a signal at room temperature measurements and its appearance at 77 K confirms that the signal with $g = 4.27$ has to be attributed to Mn^{2+} ions, which are present in another phase characterized by a high electrical conductivity at room temperature and a low one at 77 K (see Section 3.1.3).

3.2.3. Relationship between varistor formation and changes of the EPR signal

The mixtures used for the synthesis of varistors ceramics may be divided into three basic groups:

(i) the mixtures obtained using ZnO powders (a, d);

(ii) the mixture prepared using ZnO in the form of soluble salts and melts (c, e);

(iii) the mixture prepared by a combination of the previous two methods (b).

3.2.3.1. Varistor mixtures a and d. After the calcination the particles consist of a ZnO core surrounded by a homogeneous layer of corresponding oxides. Due

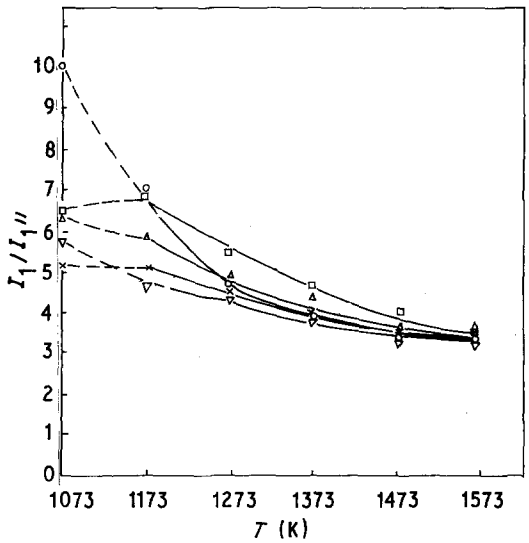

Figure 6 The ratio between amplitude singularities (1 and 1″) in EPR spectrum of Mn^{2+} in ZnO as the function of sintering temperatures for the investigated systems. Symbols as in Fig. 2.

to the dehydration processes which occur during the calcination the mixtures a and d must contain very finely dispersed homogeneous particles. The increase of temperature of thermal treatment (sintering and partially calcination) initiates both solid state reactions between various components in the layer and between ZnO and these components. It was found that the addition of NaOH into the mixture of additives inhibits the entry of Mn^{2+} ions into the ZnO lattice. The value of $I_{Mn^{2+}}$ of mixture a is higher than in the case of mixture d in practically the whole range of sintering temperatures (Fig. 4). Mn^{2+} ions, however, in mixture a are in more deformed places of the ZnO lattice, especially in the case of sintering temperatures 1073 to 1273 K. It seems that the defect state of the surroundings of Mn^{2+} ions, which enter into the ZnO lattice at low sintering temperatures, depends on the defect state of the initial ZnO particles. Manganese can also, however, enter into the ZnO lattice as ions with a valency higher than +2. This means that in the case of mixture d, Na^+ ions play the role of compensating impurity. Defect states of ZnO particles represent the localization places of Mn^{3+}–Na^+ i.e. the part of the manganese ion which contributes to the EPR signal of defect state of mixture a, in the case of mixture d is present as Mn^{3+} and does not affect the EPR signal of defect states of mixture a, in the case of mixture d is the result of Mn^{2+} presence in the perfect surroundings of ZnO. Surface complexes of the type Mn^{3+}–Na^+ may inhibit the entry of Mn^{2+} ions from the layer of additive mixtures into the ZnO particles.

With the increase of sintering temperature the layer of ZnO particles containing Na_2O takes part in the formation of phases with other additive oxides. At the same time the lower content of surface complexes Mn^{3+}–Na^+ contributes to the diffusion of Mn^{2+} ions in ZnO particles. The signal intensity $I_{Mn^{2+}}$ in systems a and d becomes equal.

The extreme character of the temperature change of signal amplitude with $g = 4.27$ (Fig. 7) is the result of the nature of the process of electroconductive phase formation. With the rise of sintering temperature the content of this phase is increased. It becomes ordered and a recovery of defects occurs causing the enlargement of signal amplitude. The consequent decrease of intensity may be connected with the evaporation or the dissolution of the formed phase in ZnO, and is confirmed by the increase of Mn^{2+} signal intensity in ZnO (Fig. 4).

It is interesting to note the difference between the amplitude changes ($g = 4.27$) of mixtures a and d (Fig. 7). In the case of mixture a the maximum intensity was reached at 1173 K, but for mixture d the same effect was obtained at 1373 K. The presence of Na_2O contributes to temperature stability of the electroconductive phase.

3.2.3.2. Varistor mixtures c and e. The main advantage of the dissolution method used for the preparation of mixture c compared to mixture a lies in the possibility of a more homogeneous distribution of the same volume of additive mixture across the basis finer than the initial ZnO particles. EPR data indicate that such

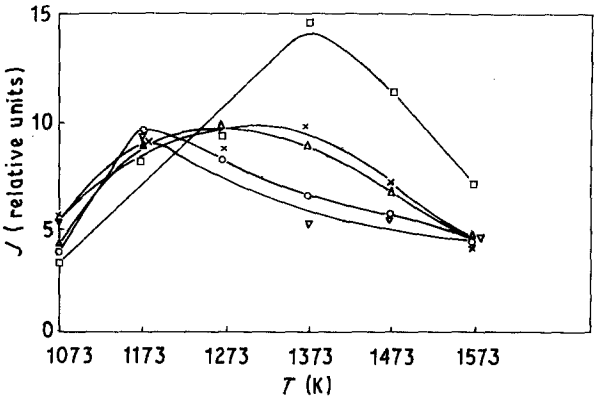

Figure 7 EPR signal amplitudes with $g = 4.27$ as the function of sintering temperatures of the investigated systems ($T_{meas} = 77$ K). Symbols as in Fig. 2.

particles have a more ordered structure resulting in more difficult entry of Mn^{2+} ions at sintering temperature range 1073 to 1173 K.

The method used for the preparation of mixture e enables a mixture which is homogeneous at the atomic level to be obtained. The intensity $I_{Mn^{2+}}$ of the samples sintered at 1073 K is much higher than the values obtained in the case of other mixtures. At the same time, the intensity of the signal with $g = 4.27$ is also the highest.

Similar values of $I_{Mn^{2+}}$ for the sample prepared using other methods (Fig. 4) indicate that Mn^{2+} concentration in ZnO is limited by their solubility at a given temperature and is determined by the conditions of synthesis. The behaviour of the signal with $g = 4.27$ which results from the electroconductive phase (Fig. 7) is similar because the electroconductive phase is formed from the oxides insoluble in ZnO whose content is practically equal in all methods used.

3.2.3.3. Varistor mixture b. The method used for the preparation of mixture b is a combination of methods a and c. It is characteristic for this case that the EPR signal of Mn^{2+} in ZnO changed with temperature (Figs 4 and 7). The Mn^{2+} surroundings in ZnO was more perfect than could be expected and is the consequence of the differences in precipitation conditions.

4. Conclusion

The use of paramagnetic Mn^{2+} ions as additives in the preparation of ZnO varistors enables the application of the EPR technique for the study of structural aspects of varistor formation during sintering. Qualitative and quantitative changes in the EPR signal are the result of sintering kinetics and is responsible for the final properties of the varistors. The entry of Mn^{2+} ions into the ZnO lattice ($g = 2.001$) is dependent, not only on the solubility of manganese in ZnO at a given temperature, but also on other parameters like the sintering time, the defect structure of ZnO powders and additives, the particle sizes and the presence of other additives. The Mn^{2+} signal in the electroconductive phase ($g = 4.27$) coincides with the law of its formation and its consequent disappearance. Although in this paper little attention has been paid to the analysis of the electroconductive characteristics of

different phases in varistors, the possibilities for future work are large. The possibilities of the EPR method may be enlarged by the use of ionization, initiating, for example, the capture of electrons by means of anion vacancies (the formation of paramagnetic colour centres) or valance changes of the type $Mn^{2+} \rightarrow Mn^{3+}$.

The consideration of various technological aspects of the formation of multiphase ZnO ceramics with non-linear properties emphasizes once more the great possibilities for the production of materials with predicted properties on the basis of fundamental principles. The understanding of crystallochemical transformation in this case and in similar multi-component systems requires a complex approach including quite different physical methods of analysis.

Acknowledgements

This study was carried out as a scientific cooperation between the Council of Yugoslav Academies of Sciences and the Academy of Science of Soviet Union. The research was supported by the Serbian Council of Sciences through the project "Physical Chemistry of Condensed Systems".

References

1. J. E. WERTZ and R. J. BOLTON, "Electron spin resonance - Elementary theory and practical applications" (McGraw-Hill, New York, 1972).
2. A. CARRINGTON and A. D. McLACHLAN, "Introduction to magnetic resonance with applications to chemistry and chemical physics" (Harper Row, New York, 1967).
3. G. V. SAMSONOV, M. V. VLASOVA, N. G. KAKAZEY, B. GRIGORYEV, D. P. USKOKOVIĆ and M. M. RISTIĆ, *J. Physique* **37** (1976) C7-415.
4. M. V. VLASOVA, N. G. KAKAZEY, P. KOSTIĆ, O. MILOSEVIĆ and D. P. USKOKOVIĆ *J. Mater. Sci.* **20** (1985) 1160.
5. R. J. LAUF and W. D. BOND, *Amer. Ceram. Soc. Bull.* **63** (1984) 278.
6. E. SONDER, T. C. QUINBY, and L. KINSER, *ibid.* **64** (1985) 665.
7. O. MILOSEVIĆ, D. POLETI, Lj. KARONOVIĆ, V. PETROVIĆ and D. USKOKOVIĆ, Second International Varistor Conference, Schenectady, USA, 1988, in (The American Ceramic Society, Ohio, USA, 1989).
8. R. G. DOSCH, in "Science of Ceramic Chemical Processing", edited by L. L. Hench and D. R. Ulrich (John Wiley, New York, 1986).
9. E. IVERS-TIFFEE and K. SEITZ, *Amer. Ceram. Soc. Bull.* **66** (1987) 1384.
10. K. SEITZ, E. IVERS-TIFFEE, H. THOMANN and A. WEISS, VI World Conference on High Tech. Ceramics, Milano, 1986, in High Tech. Ceramics, edited by P. Vincenzini (Elsevier, Amsterdam, 1987).
11. YA. G. KLYAVA, EPR Spektroskopiya blizhnego poryadka i ego narusheniye v kristallicheskih i stekloobraznih tverdyh telah, Avtoref. dissert. doktora fiz.-mat.nauk, Salaspilo, 1984.
12. M. V. VLASOVA, S. I. GORBACHUK, N. G. KAKAZEY and V. M. MELJNIK, *Physika i technika visokih davlenii,* **18** (1985) 77.
13. C. HAUSER and B. RENAUD, *Phys. Status Solidi a* **10** (1972) 161.
14. M. V. VLASOVA, S. I. GORBACHUK, N. G. KAKAZEY and M. M. RISTIĆ, *J. Mater. Sci.* **18** (1983) 245.
15. G. M. ZHIDOMIROV, Ya. S. LEBEDEV and S. M. DOBRYAKOV, "Interpretaciya slozhnih spektrov EPR", (Nauka, Moscow, 1975).
16. C. KITTEL and E. ABRAHAMS, *Phys. Rev.* **90** (1953) 238.
17. J. KORRINGA, *Physica* **19** (1950) 601.
18. N. N. TIHOMIROVA, S. M. DOBRYAKOV and I. V. NIKOLAEVA, *Phys. Status Solidi a* **10** (1972) 593.

Received 26 January 1989
and accepted 26 January 1990